Robot for decontamination with 3D move on sensing

CUI Yu[1], LI Xiang[1], MINAMI Mamoru[1], YANOU Akira[1], YAMASHITA Manabu[2], and ISHIYAMA Shintaro[3]

1. Graduate School of Nature Science and Technology, Okayama University, 3-1-1 Tsushima-naka, Kita-ku, Okayama-shi, Okayama-ken, 700-8530, Japan (CUI: paz177d4@s.okayama-u.ac.jp, LI: p61a36vz@s.okayama-u.ac.jp, MINAMI: minami-m@cc.okayama-u.ac.jp, YANOU: yanou-a@cc.okayama-u.ac.jp)

2. ISHIGAKI COMPANY, LTD, 1-1-1 Kyobashi, Tsyu-ouku, Tokyo, 104-0031, Japan (manabu.yamashita@ishigaki.co.jp)

3. Japan Atomic Energy Agency. 2-4 Shirakatashirone, Tokai-mura, Naka-gun, Ibaraki pref. 319-1195, Japan (ishiyama.shintaro@.jaea.go.jp)

Abstract: Toward reconstruction of Tohoku region in Japan devastated by nuclear disaster, decontamination work has been progressing. But a large volume of collected contaminated soil is waiting for decontamination at temporarily-constructed custody facilities. Since the volume of stored soil is huge, the task to reduce the volume of contaminated soil using dehydrator machine called Filter Press (FP) appears to be important. The task to reduce the soil volume means that separation of concentrated radioactive soil and decontaminated clean soil for returning to the place where the soil is gathered. Having radioactive soil concentrated has a good facet of reducing the volume of radiative substances, it also brings a risk that the workers for the FP should be exposed to radiations. As measures to reduce radiation exposure of workers to zero, the FP should be redesigned into full automatic machine system, requiring robots that enable visual controlled task with "3D Move on Sensing (3D-MoS)." In this study, based on the model including attribute information such as color and shape of the target object, the robot can detect target pose automatically by 3D-MoS. And then, the 3D-MoS system has been proved to be valid for decontamination task, *i.e.*, removing the cloth of FP even though the position of components of FP be uncertain.

Keyword: decontamination robot; visual serving; filter press

1 Introduction[1]

After the Tohoku Earthquake on March 11, 2011, in Fukushima Prefecture, which brought tsunami and nuclear power accident, a large amount of accumulated contaminated soils has been left. And in recent years there has been increasing attention to the technology to decontaminate the soil. Therefore one of the authors, Ishiyama [1-4] has confirmed that the FP has the abilities to separate soil concentrated radioactive substances and decontaminated remains. Even though radiation of concentrated soil is not high, but we need robotized operation for the FP, particularly the exchanging task of the filter cloth that accumulates the radioactive contaminated substances.

General 3D vision for recognition with dual-eye system uses epipolar geometry for sensing 3D positions of the objects, which must meet a condition that the points on the 3D target object has to correspond to the points on camera images, otherwise calculated pose of object includes errors, when it calculates 3D pose from 2D images---inverse kinematic (2D information is expanded to 3D).

Contrarily to the current epipolar-geometry-based 3D vision, proposed 3D-MoS has a vital difference, *i.e.*, it uses forward kinematic (3D information is contracted to 2D). That is, (1) a model made of 3D shape and color is defined, (2) assume the 3D pose of target, (3) the shape of target model is projected into cameras' images by using assumed 3D pose, (4) if the target models projected into dual-eye-camera images should be completely matched to the real target in the images, the assumed pose of the 3D target can be thought to be identical to the pose of real object in 3D space, meaning the pose of real target has been found [5-7]. So the authors applied the 3D-MoS for filter cloth replacement task shown in Fig.1.

Received date: June 16, 2015
(Revised date: August 5, 2015)

Fig. 1: Two 3D-MoS robot system with dual hand-eye cameras set beside filter press decontamination machine for full automatic exchanging of cloths of filter press.

In this study, based on the attribute information (multi-function sensing), such as color and shape of the object, automatic robotic system has been developed for replacing filtering clothes that concentrate radioactive substances, enabling workers to avoid being exposed to radiation.

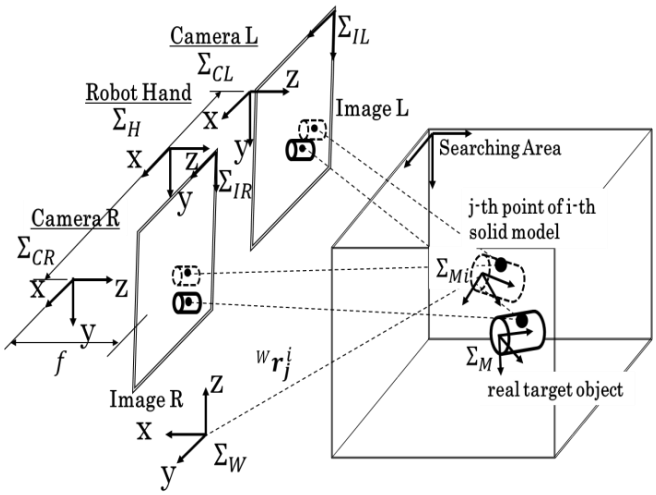

Fig.2 Coordinate system of dual eyes---whose two cameras are set at the hand (represented by Σ_H) of robot---are defined as Σ_{CL} and Σ_{CR}. The coordinates of camera images are Σ_{IL} and Σ_{IR}, in which real target object defined by Σ_M and i-th solid model defined by Σ_{Mi} are projected from the 3D space depicted at right side.

2 Pose recognition method

2.1 Kinematics of stereo-vision

We utilize perspective projection as projection transformation. Fig. 2 shows the coordinate system of the dual-eyes vision system. The target object's coordinate system is represented by Σ_M, the i-th solid model coordinate system is represented by Σ_{Mi} and image coordinate systems of the left and right cameras are represented by Σ_{IL} and Σ_{IR}. Σ_W means world coordinate systems and Σ_H dose hand coordinate systems of the robot.

The j-th point on the i-th model can be described using these coordinates and homogeneous transformation matrices. At first, a homogeneous transformation matrix from right camera coordinates, Σ_{CR} to Σ_{Mi} is defined as ${}^{CR}\boldsymbol{T}_{Mi}$. And the j-th point on the i-th model in Σ_{CR} and Σ_{Mi} is defined as ${}^{CR}\boldsymbol{r}_j^i$ and ${}^{Mi}\boldsymbol{r}_j$. Then ${}^{CR}\boldsymbol{r}_j^i$ is,

$$ {}^{CR}\boldsymbol{r}_j^i = {}^{CR}\boldsymbol{T}_H\,{}^{H}\boldsymbol{T}_W(\boldsymbol{q})\,{}^{W}\boldsymbol{T}_{Mi}({}^{W}\boldsymbol{\phi}^i)\,{}^{Mi}\boldsymbol{r}_j, \qquad (1) $$

where ${}^{Mi}\boldsymbol{r}_j$ is predetermined fixed vectors, ${}^{CR}\boldsymbol{T}_H$ is fixed matrix, ${}^{H}\boldsymbol{T}_W$ is determined by robot's joint angle vector $\boldsymbol{q}$, and ${}^{W}\boldsymbol{T}_{Mi}$ is determined by assumed position and orientation, which are usually called as pose of the i-th model ${}^{W}\boldsymbol{\phi}^i$.

The position vector of the j-th point in right image coordinates is described as ${}^{IR}\boldsymbol{r}_j^i$ by using projection matrix $\boldsymbol{P}$ of camera as,

$$ {}^{IR}\boldsymbol{r}_j^i = \boldsymbol{P}\,{}^{CR}\boldsymbol{r}_j^i. \qquad (2) $$

By the same way as above,

$$ {}^{CL}\boldsymbol{r}_j^i = {}^{CL}\boldsymbol{T}_{Mi}\,{}^{Mi}\boldsymbol{r}_j, \qquad (3) $$

$$ {}^{IL}\boldsymbol{r}_j^i = \boldsymbol{P}\,{}^{CL}\boldsymbol{r}_j^i. \qquad (4) $$

Then position vectors projected in the Σ_{IR} and Σ_{IL} of arbitrary j-th point on target object can be described as ${}^{IR}\boldsymbol{r}_j^i$ and ${}^{IL}\boldsymbol{r}_j^i$. Then equation (2) and equation (4) are rewritten as,

$$ {}^{IR}\boldsymbol{r}_j^i = \boldsymbol{f}_R({}^{W}\boldsymbol{\phi}^i, {}^{Mi}\boldsymbol{r}_j, \boldsymbol{q}), \qquad (5) $$

$$ {}^{IL}\boldsymbol{r}_j^i = \boldsymbol{f}_L({}^{W}\boldsymbol{\phi}^i, {}^{Mi}\boldsymbol{r}_j, \boldsymbol{q}). \qquad (6) $$

These relations connect the defined points, ${}^{Mi}\boldsymbol{r}_j$, on the 3D object and projected points on the left and right images, since the joint angle vector of robot, $\boldsymbol{q}$,

can be detected by robot, ${}^{IR}\boldsymbol{r}_j^i$ and ${}^{IL}\boldsymbol{r}_j^i$ could be calculated when the value of ${}^{W}\boldsymbol{\phi}^i$ is given by an assumption in GA process mentioned in next subsection.

2.2 Recognition method based on genetic algorithm

The real filter cloth rod with color and shape information used in this paper is shown in Fig. 3.

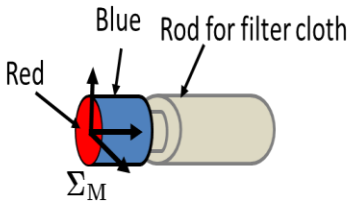

Fig.3 Shape of the rod of filter cloth and the color put on end-surface(red) and side-surface(blue).

The pose of the rod are represented by the coordinate systems, Σ_M, which is fixed at the rod, where the color of the end-surface is red and of the side-surface is blue. The other rods with different color and same shape also are prepared. Though the rods have the same shape, they can be recognized as different target by the color information. A robot system is constituted as shown in Fig. 4, where two robots are face-to-face. This is for the two robots to operate harmoniously to grasp both sides of a single rod and to remove it for changing filter cloth. To recognize the same rod correctly, the rod color is significant.

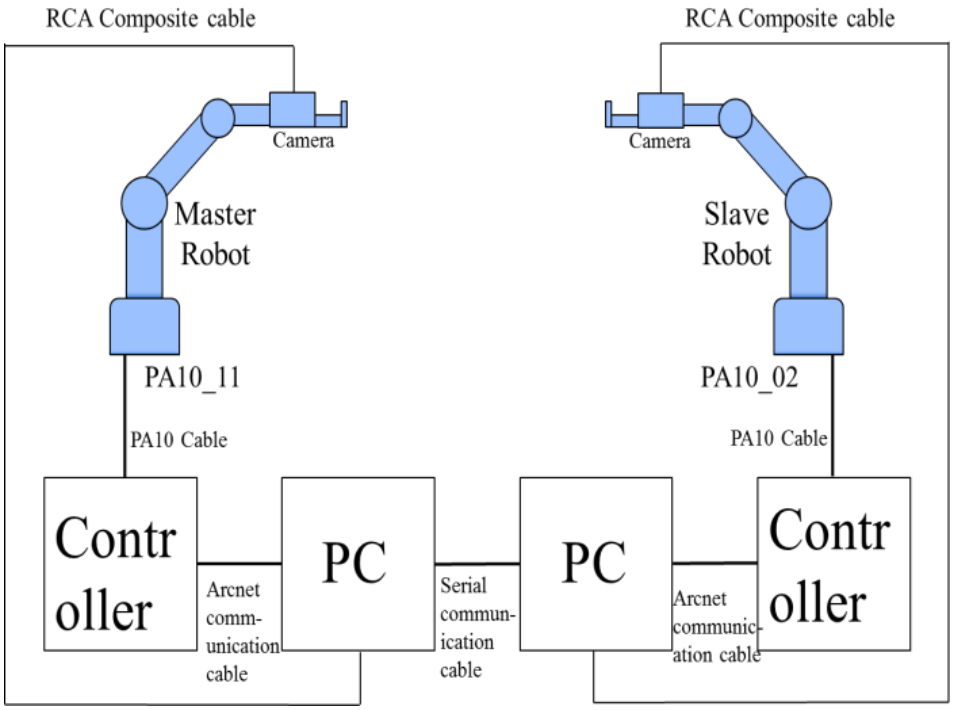

Fig.4 Two robots system tasked with conducting coordinated operation to grasp a single rod and to remove it for changing filter cloth.

In order to measure the pose of a real rod, many solid models having the same shape and color with the real rod but having different poses are prepared. The state that the i-th solid model and the real rod exist in 3D space is shown in Fig. 5(the right side). The pose of the i-th solid model is represented as ${}^{W}\boldsymbol{\phi}^i = [\boldsymbol{t}_x^i, \boldsymbol{t}_y^i, \boldsymbol{t}_z^i, \varepsilon_1^i, \varepsilon_2^i, \varepsilon_3^i]$ ($\varepsilon = [\varepsilon_1^i, \varepsilon_2^i, \varepsilon_3^i]$ is quaternion posture parameter) in Σ_W. The six elements of ${}^{W}\boldsymbol{\phi}^i$ is expressed in binary with 12 bits. The shape and color of the solid model and the real rod projected to right camera image are shown in Fig. 5.

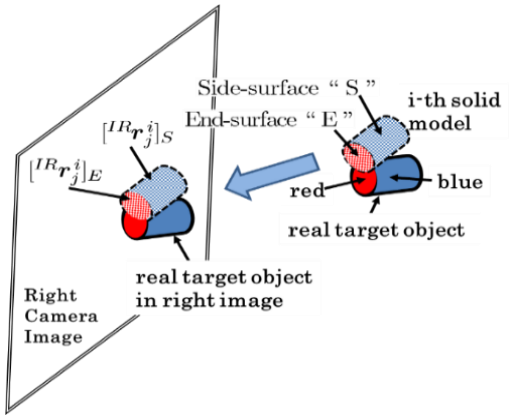

Fig.5 i-th object model projected to right image plane whose end-surface part denoted by "E" and side part denoted by "S." Projected points ${}^{IR}\boldsymbol{r}_j^i$ on "E" are represented as $[{}^{IR}\boldsymbol{r}_j^i]_E$ and on "S" as $[{}^{IR}\boldsymbol{r}_j^i]_S$

Then a correlation function representing a matching degree of projected model against the real rod in the image is used as a fitness function in GA process. When the pose of the model and that of the real rod are identical, the fitness function value is to be maximized. We have confirmed that a correlation function having a highest peak with a condition of the pose of real target completely being identical to a model could be designed [6], [7]. So the problem of recognition for target object can be changed into an optimization problem that explores the maximum of fitness function and finds the ${}^{W}\boldsymbol{\phi}^i$ to give the maximum.

There are many methods for the exploration of maximum of functions. The easiest method is full exploration that calculates all function value and find the maximum, which takes too much time. It is significant to shorten time during recognition, so in this research GA, which can find the maximum more efficiently in shorter time, is used to solve it.

2.3 The definition of fitness function

${}^{IR}\boldsymbol{r}_j^i$ and ${}^{IL}\boldsymbol{r}_j^i$, got by equation (5) and (6), are calculated by fixed points ${}^{Mi}\boldsymbol{r}_j$ of the surface of the i-th solid model and the pose ${}^{W}\boldsymbol{\phi}_k^i$, which is at the k-th evolving generation of the i-th model in GA process. As shown in Fig. 5, the point group of the end-surface "E" in right camera image projected from solid model is defined as $[{}^{IR}\boldsymbol{r}_j^i({}^{W}\boldsymbol{\phi}_k^i)]_E$, and by the same way the side-surface one is defined as $[{}^{IR}\boldsymbol{r}_j^i({}^{W}\boldsymbol{\phi}_k^i)]_S$.

If the red-hue value of a point at position $\boldsymbol{r}$ in right camera image, exists in a predetermined specified range, the value of a function $\boldsymbol{F}_R(\boldsymbol{r})$ takes "1," else the value is "0." Here, as shown in Fig. 3, the end-surface of the cylindrical target is red and the side-surface is blue. So $\Sigma_j \boldsymbol{F}_R([{}^{IR}\boldsymbol{r}_j^i({}^{W}\boldsymbol{\phi}_k^i)]_E)$ means the number of points that the end-surface of the cylindrical model in the right camera image overlaps the red section of the end-surface of the real target in right camera image. By the same way $\Sigma_j \boldsymbol{F}_B([{}^{IR}\boldsymbol{r}_j^i({}^{W}\boldsymbol{\phi}_k^i)]_S)$ is a function to output sum of points that overlaps the blue section of the side-surface of the real target. The ranges of hue value of red and blue are set as 30<blue<60 and 150<red<180 in this experiment. The number of total points on the end-surface is defined as qe, and the side-surface one is qs. Based on genes ${}^{W}\boldsymbol{\phi}_k^i$ of the solid model, the fitness function of red end-surface and blue side-surface $\boldsymbol{F}_{RB}({}^{W}\boldsymbol{\phi}_k^i)$ can be calculated as below:

$$\begin{aligned}\boldsymbol{F}_{RB}({}^{W}\boldsymbol{\phi}_k^i) = \frac{1}{2(\boldsymbol{q}_E+\boldsymbol{q}_S)} & \left[\left\{\sum_{j=1}^{q_E}\boldsymbol{F}_R([{}^{IR}\boldsymbol{r}_j^i({}^{W}\boldsymbol{\phi}_k^i)]_E)+\right.\right. \\ & \left.\left.(\sum_{j=1}^{q_S}\boldsymbol{F}_B([{}^{IR}\boldsymbol{r}_j^i({}^{W}\boldsymbol{\phi}_k^i)]_S)\right\}+\right. \\ & \left\{\sum_{j=1}^{q_E}\boldsymbol{F}_R([{}^{IL}\boldsymbol{r}_j^i({}^{W}\boldsymbol{\phi}_k^i)]_E)+\right. \\ & \left.\left.\sum_{j=1}^{q_S}\boldsymbol{F}_B([{}^{IL}\boldsymbol{r}_j^i({}^{W}\boldsymbol{\phi}_k^i)]_S)\right\}\right] \\ & = \boldsymbol{F}_{RB,R}({}^{W}\boldsymbol{\phi}_k^i)+\boldsymbol{F}_{RB,L}({}^{W}\boldsymbol{\phi}_k^i) \end{aligned} \quad (7)$$

$\boldsymbol{F}_{RB,R}({}^{W}\boldsymbol{\phi}_k^i)$ is a fitness function about overlap ratio between model with red end-surface and blue side-surface whose pose defined by the i-th gene in right camera image and real target. And $\boldsymbol{F}_{RB,L}({}^{W}\boldsymbol{\phi}_k^i)$ is the left one.

$\boldsymbol{F}_{RB}({}^{W}\boldsymbol{\phi}_k^i)$ scores high value on the condition that the model designated by ${}^{W}\boldsymbol{\phi}_k^i$ overlaps real target with red end-surface and blue side-surface, on the other hand it takes low value with other color information even though the model's pose coincides with target one's. So it is sure to prevent mistakes of recognition.

Because $F_{RB}({}^{W}\phi_k^i)$ is calculated from 3D shape ${}^{Mi}r_j$ and color based on ${}^{W}\phi_k^i$, it can be sure that the corresponding points in left ${}^{CL}r_j^i$ and right camera image ${}^{CR}r_j^i$ are identical. Therefore, it is impossible that the identity error happens---meaning that the i-th point of solid model in 3D space corresponds correctly to the point in right camera image and that in left.

2.4 Exploration for optimal solution with GA

The evolution process in GA is shown in Fig. 6. Models of target object where poses are represented by genes are scattered in the search space at first, then the models are intended to converge to real target as evolution progressing.

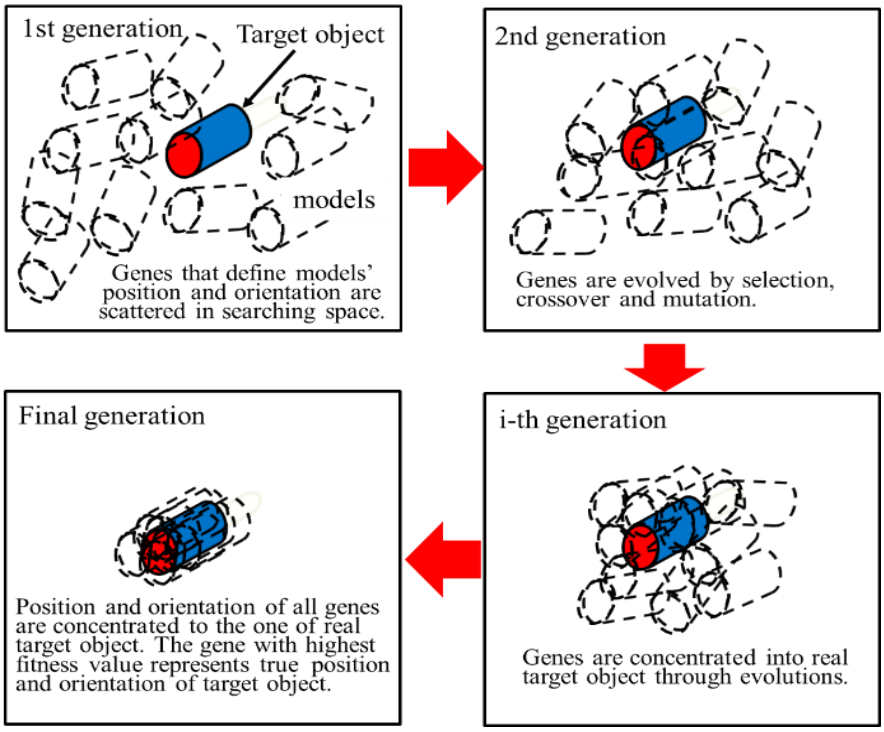

Fig.6 Evolution process, representing that 3D models converge into real target object, by matching true target object projected into 2D image plane and 3D models projected into the same plane, through evaluations on fitness function defined by equation (7).

Firstly, the 1st generation of individual of GA genes is generated in the 3D space randomly. Secondly, every individual's fitness is calculated, and then based on the calculated result, selection of the genes with high fitness value is conducted by sorting the order of genes from high to low as shown in Fig. 7. Genes in the next generation are regenerated from the selected genes through crossover and mutation like changing of generation of living things.

As shown in Table 1, selection rate is defined as 0.4, so 40% genes of last generation are used for remaking next genes in every evolution. The other parameters are shown in Table 1. The optimization abilities of GA depend on the parameters' value. Those parameters listed in Table 1 were determined through our previous visual servoing experiments [5], [7] in a try-and-error manner experimentally. Calculation time of one generation is 1.7[ms]. The fitness function value increases while evolution process progressing, making the models converge to the real target in 3D space as shown in Fig. 6. In final generation, after both the highest fitness value and the average value become high, the gene ${}^{W}\phi_k^i$ that gives the highest fitness value can be thought to represent true pose of real target.

Table 1 Parameters of genetic algorithm

Population size	20 individuals
Selection rate	0.4
Mutation rate	0.3
Length of individual	12 bits
Crossover	Two-point
Elitist model	yes
Calculation time	1.7[ms]/generation

3 Verification experiment

3.1 Machinery system for experiment

In order for removing operation of the filter cloth rod from FP, a robot that has a hole at hand to grasp the rod of FP is used as shown in Fig. 8. The robot is PA-10 made by Mitsubishi Heavy Industries. Two cameras are FCB-IX11A with 30fps video rate made by SONY.

The experiment test system composed of 3D-MoS controlled robot and filter cloth rod is shown in Fig. 9. The cameras' sight lines are fixed so that those crosses at one point in space---and that those cross point can be finely adjusted by using the DOF of camera rotation. In order to conduct removal operation of filter cloth rod, a half-cylinder-shaped hand shown in right side of Fig. 8 is installed at the tip of the robot hand.

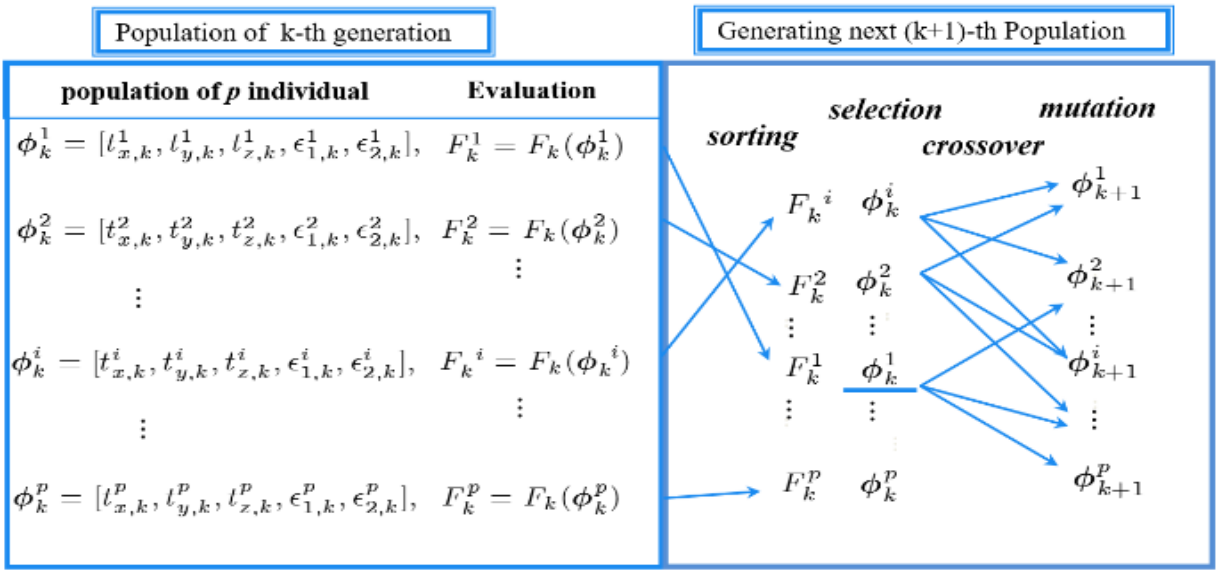

Fig.7 Evolution Process of Genetic Algorithm.

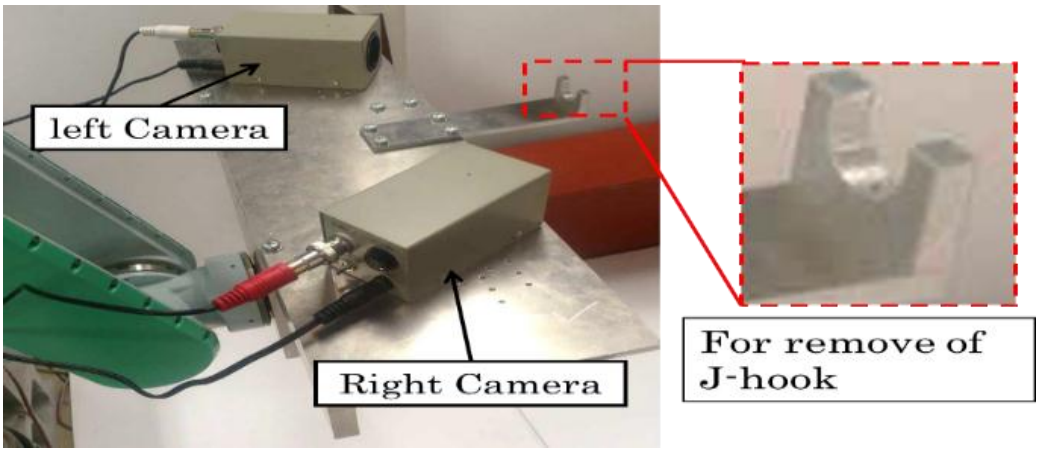

Fig. 8 3D-MoS sensor set at robot hand and its attachment for interdigitation test.

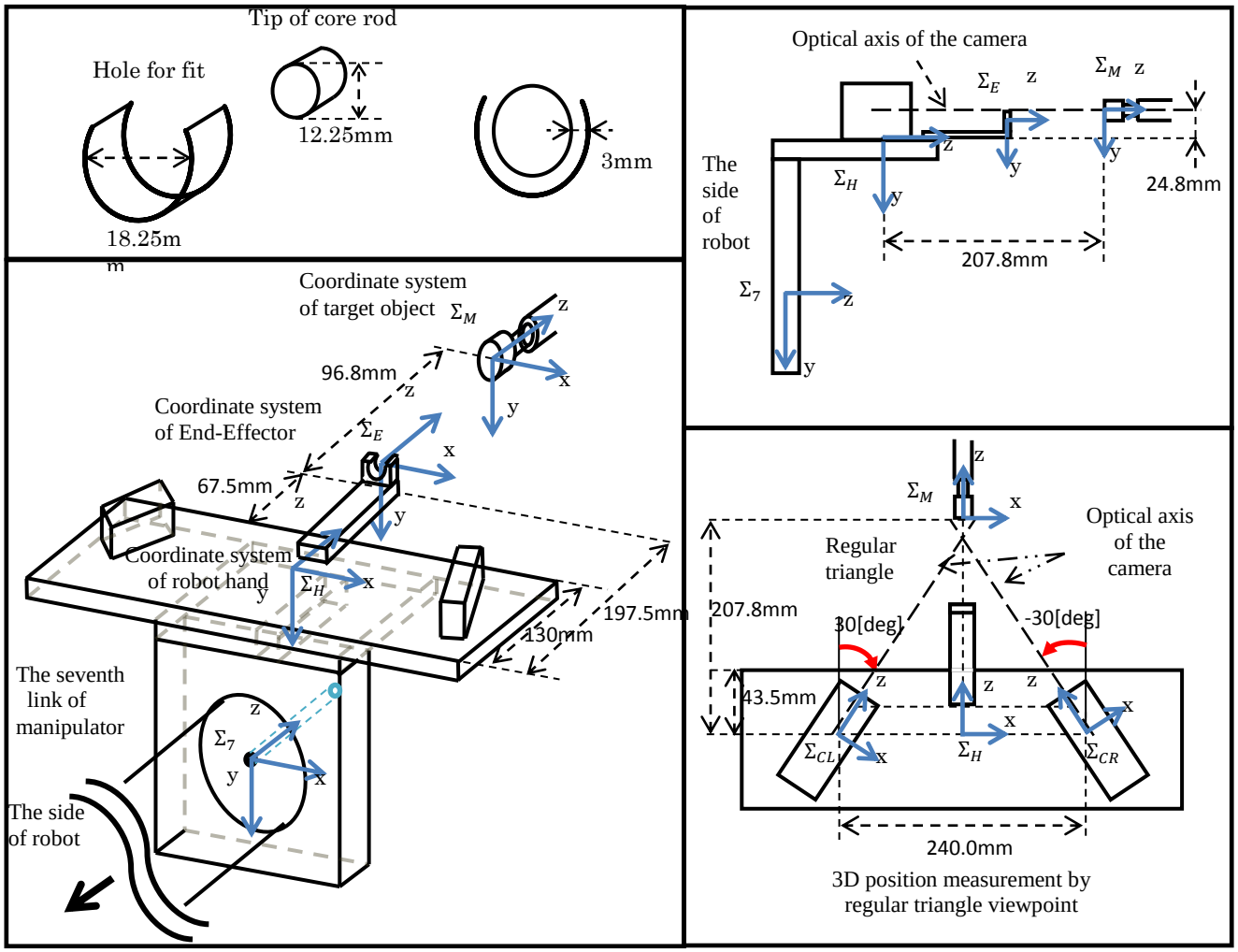

Fig.9 Experiment test composition of 3D-MoS controlled robot and rod of filter press.

3.2 Experiment condition

To perform replacement tasks of the filter cloth, the necessary steps are as follows.

1. Grasp of the filter cloth rod by half-cylinder hand using 3D-MoS as shown in Fig. 10(a)
2. Remove the filter cloth rod from the hook
3. Pull out filter cloth from the sprocket as shown in Fig. 10(b)

Because the position of the filter cloth rod is uncertain since the high pressure for filtering process deforms the shape of the filtering chamber, it is necessary to measure relative pose difference by 3D-MoS between the robot hand and the target rod. Moreover the filter cloth replacement used to be handled simultaneously by two workers at both side of a single rod before the robotic automation has been established. And the position could not be predetermined because of the deformation of the filter chamber component caused by high filtering pressure. Therefore, in order to achieve to grasp the filter cloth rod, a system that can find the 3D position of target rod based on the camera image was inevitable. In this experiment, in order to verify the recognition accuracy of the GA with camera images, repeated recognition experiments were conducted. In addition, based on the recognition result of the rod, we confirmed whether the hand can grasp the filter cloth rod. After having confirmed that the both robots have removed the rod successfully, the two robots grasp the upper end rod of the cloth shown in Fig. 10(b). Then pulling up operation of the cloth rod by the two robots is conducted in a coordinated manner using communication network.

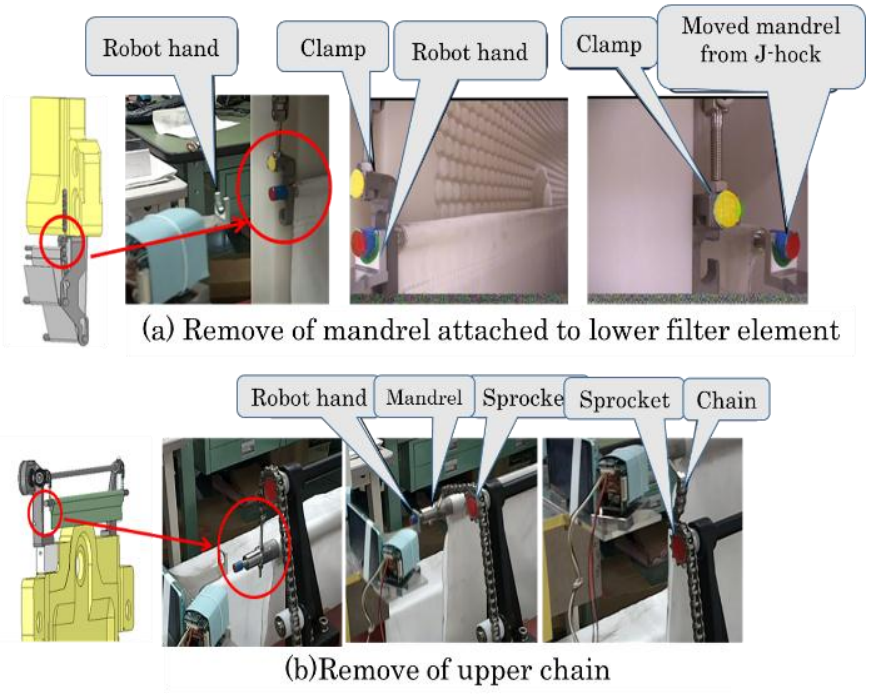

Fig. 10 Remove of filter element from filter press.

In Fig. 11 the relationship between Σ_W, that is the world coordinate system of the manipulator and Σ_H that is the hand coordinate system is shown. And in Fig. 9, the hand coordinate system Σ_H and the end effector coordinate system Σ_E are defined. Left camera is tilted clockwise 30 [deg] around the y axis of the coordinate system Σ_H, while the right camera is tilted 30 [deg] counterclockwise as shown in lower-right part of Fig. 9.

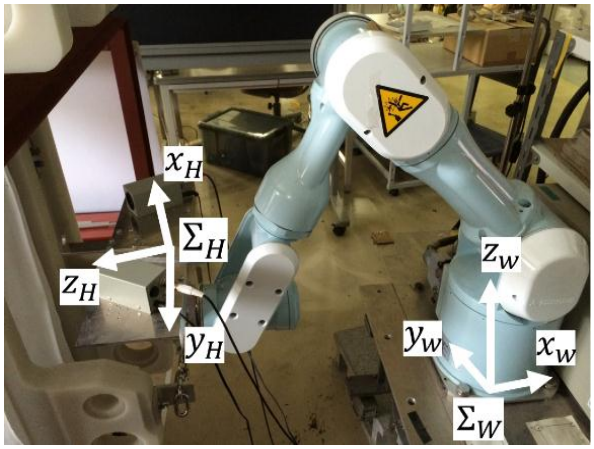

Fig. 11 Coordinate systems of 3D-MoS robot.

3.3 1000 times recognition experiment

To investigate the recognition accuracy of rods using the proposed method, recognition experiments were carried out 1000 times, and the error of the recognition results were analyzed. The rod is installed at the position (x, y, z) = (0, -24.8, 207.8) [mm] based on Σ_H, where the point is an intersection of the optical axes of left and right cameras, which are depicted in the positional relations among coordinates in right-hand side of Fig. 9. And then the recognition experiment was conducted. The radius of the hole installed at the top of the hand is 9.125[mm], and that of the filter cloth rod is 6.125[mm]. Therefore, there is 3[mm] gap at the vertical and horizontal directions (x, y direction in Σ_E). For the depth direction (z direction in Σ_E), the length of the recognized part of filter cloth core rod is 16[mm] and the depth of the hole is 5[mm]. In order to make the removal easier, it is expected that the hand should reach the middle of the recognized part of the core rod after inserting, so the recognition error should be less than 3[mm]. To accomplish the inserting and removing, the error in each direction (x, y, z) should be always kept less than 3 [mm].

3.4 1000 times inserting experiment

Based on the results of 1000 times recognition

experiments, 1000 times inserting experiments have been done. In order to create the condition that the positions of the filter cloth rod are unknown, the position of the hand is changed randomly at the beginning of every measurement. Initial position of the manipulator is (x, y, z) = (0, -24.8, 207.8), which is the intersect point of the optical axes of left and right cameras based on Σ_H. 1000 times inserting experiment procedure is below.

1. Manipulator moves randomly under the range of 10mm in each direction (x, y, z) from starting position (0, -24.8, 207.8), that has the hand position deviate from the point of intersection of the optical axes of left and right cameras. (The deviation of robot hand of 10[mm] or less are given as a condition of randomness of the hand position error, which is justified by the positioning accuracy of FP.)
2. Recognition of filter cloth rod according to the camera image (the first time recognition) is conducted, and detect the pose error between $\Sigma_{\underline{M}}$ and Σ_M as shown in Fig. 12.
3. Manipulator moves in x, z directions that make (xe, ze) reduce to zero, where the hand position after the hand motion is depicted by dotted line in Fig. 12.
4. Recognition is performed again (the second time recognition)
5. If the error of direction in x, z is 2mm or less, insert the hole of robot hand into the rod based on the result of the current recognition. Otherwise repeat 2 to 5 again.
6. Return to the initial position after having completing insertion and repeat from 1.

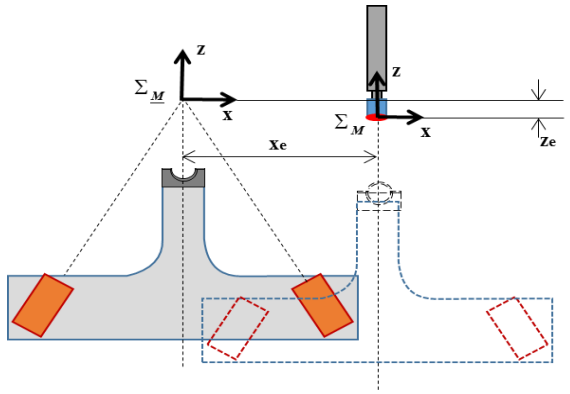

Fig. 12 The pose error between $\Sigma_{\underline{M}}$ and Σ_M.

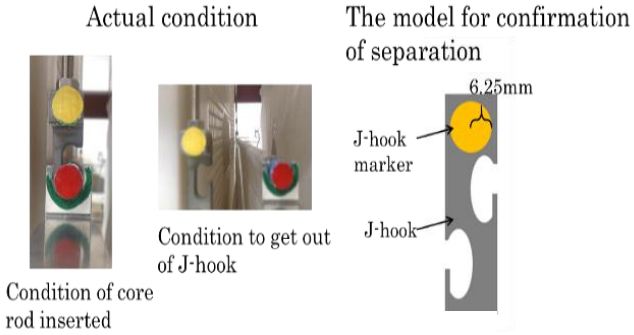

Fig. 13 J-hook model.

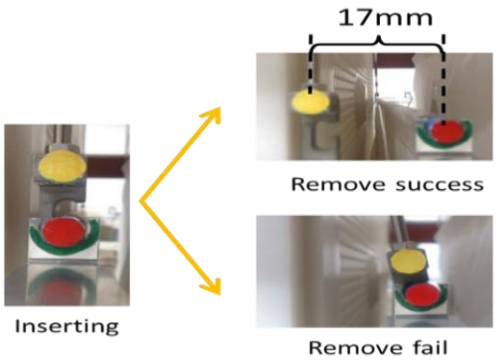

Fig. 14 Judgement about removal.

3.5 The rod removing experiment

The rod can be removed from a J-hook shown in Fig. 13 through the movement of the robot hand in left or right direction with 20[mm] after inserting. Because the objective of this system is to accomplish full automation, so it is significant to judge whether the removing has been succeeded. A yellow circle was drawn at the top part of J-hook as shown in Fig. 13. If the distance between the rod and the yellow J-hook marker is greater than 17[mm], it can be judged that removing process is successful as shown in Fig. 14.

3.6 The chain removing experiment

Before removing the chain from sprocket by a robot's hand, length of chain should be measured every time since it is not guaranteed as constant. So it is necessary to recognize the length of "a" depicted in Fig. 15. And there is also a problem that movement range of hand may not be adequate to remove chain because chain is connected to sprocket with gear. In order to remove the chain in this situation, a hand trajectory to remove is generated to make the hand follow an involute trajectory. And then the remove experiment was conducted. Sprocket model is shown in Fig. 15.

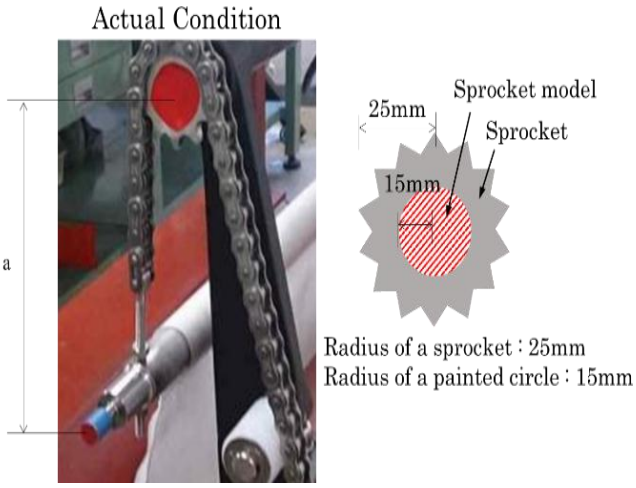

Fig. 15 The filter cloths are suspended from chain through top sprocket that make the cloths run to peel away the contaminated-concentrated and mass-reduced soil from filter cloths. It can be conducted that the FP cloths be pulled up by robots after completing the task of the chain being detached from the sprocket.

4 Experiment result

4.1 Result for recognition experiment

The result of the recognition experiment is shown in Table 2.

Table 2 True position of circular rod end, recognition error and its standard deviation when the target position (x, y, z) = (0, -24.8, 207.8)[mm] are given, which means that the cloth rods are stationarily placed at the cross point of the cameras' sight lines.

	x[mm]	y[mm]	z[mm]
average value	-0.00764	-24.746	207.7948
average recognition error	-0.00764	0.053574	-0.00523
standard deviation	0.56028	0.60226	0.99700

In this paper, $\bar{x}$, $\bar{y}$ and $\bar{z}$ indicate recognition average values and $\Delta\bar{x}$, $\Delta\bar{y}$ and $\Delta\bar{z}$ do average recognition errors. σx, σy and σz stand for standard deviations. The average value of 1000 times recognition is ($\bar{x}$, $\bar{y}$, $\bar{z}$) = (-0.00764, -24.746, 207.7948)[mm]. The error between recognition value and the true value is ($\Delta\bar{x}$, $\Delta\bar{y}$, $\Delta\bar{z}$) = (-0.00764, 0.053574, -0.00523)[mm]. Based on the results, it can be sure that the recognition errors are small. Standard deviation σx =0.56028[mm] and $\sigma\bar{y}$ =0.60226[mm], are also small, but σz =0.99800[mm] is bigger than x and y. This is because the z direction is same as the camera depth direction, in which the amount of movement of target object in camera image is small, when the relative movement along to z direction were given.

As shown from Fig. 16 to Fig. 18, the recognition errors in x direction are in a range of -1.5~1.5[mm], those in y direction are -1.5~1.7[mm] and those in z direction are -2.9~3.3[mm]. From Fig 16 and Fig. 18, it can be said that the distributions in x and z direction are similar to normal distribution. An average recognition error and its standard deviation are shown in Table 3. Generally, on the condition that data is similar to normal distribution, the probability that the data is in the range of the average $\pm 3\sigma$ is 99.7%. That means the error in x direction is less than 1.7[mm] and z direction is below 3.0[mm] with probability of 99.7%. Though data in y direction is not like normal distribution, all of data are in the range from -1.5[mm] to 1.5[mm], which meet the accuracy that below 3[mm].

So it can be concluded that the recognition accuracy in x, y ,z direction is less than 3[mm] with the probability of 99.7%.

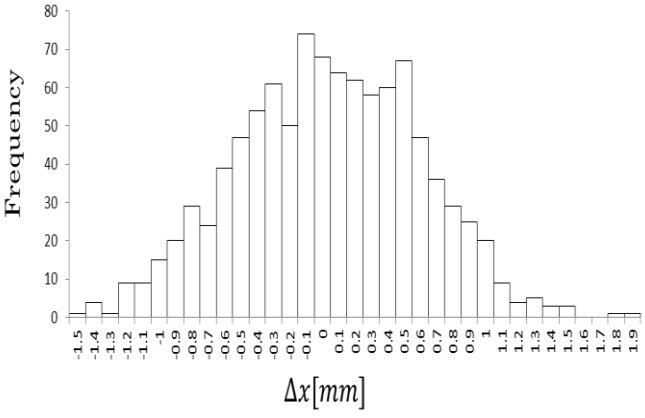

Fig. 16 Histogram of a recognition error $\Delta\bar{x}$.

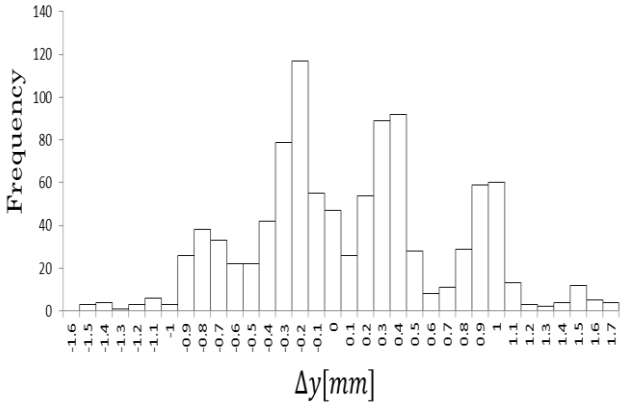

Fig. 17 Histogram of a recognition error $\Delta\bar{y}$.

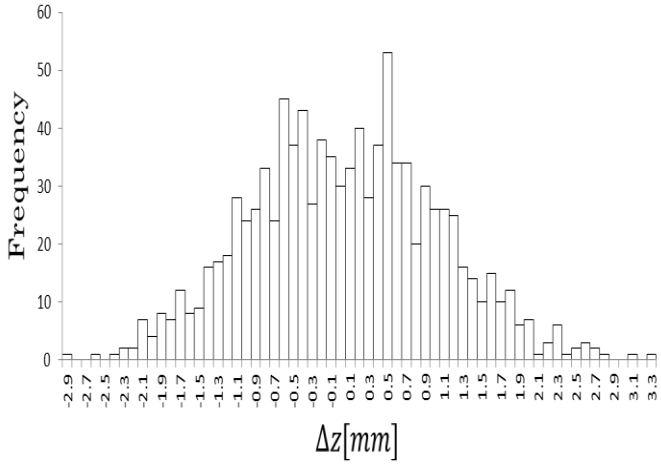

Fig. 18 Histogram of a recognition error $\Delta\bar{z}$.

Table 3 Recognition error and its standard deviation

	x[mm]	y[mm]	z[mm]
average-3 σ	-1.68847	-1.75319	-2.99622
average-2 σ	-1.12819	-1.15094	-1.99923
average- σ	-0.56791	-0.54868	-1.00223
average	-0.00764	0.053574	-0.00523
average+ σ	0.55264	0.65583	0.991762
average+2 σ	1.112916	1.258085	1.988759
average+3 σ	1.673193	1.860341	2.985756

4.2 Result for inserting experiment

After confirming that the probability of recognition is 99.7% in 1000 times recognition experiment, 1000 times inserting experiment was followed. All of inserting experiments have been succeeded. Here 1000 times inserting experiment procedure in the section 3.4 was used to heighten the recognition accuracy. The result of the second time recognition in the step 4 of 1000 times inserting experiment procedure in the section 3.4 is shown in Table 4. The deviation value of the rod in the step 1 is detected by the first recognition. From the result, the manipulator moves in x, z direction to the position where the half-cylinder hand and the rod is point-blank in the step 3, so the target rod is in the cross point of left and right cameras' optical axis during the second recognition in the step 4. In other words, the second recognition condition in 1000 times inserting experiment is same as 1000 times recognition experiment in section 3.3. Comparing the result of Table 2 and Table 4, the average error is basically same, but the standard deviation in Table 4 is bigger than Table 2. This is because the second recognition results include position errors less than 2[mm] as written in procedure 5 in subsection 3.4. This is the different condition from the experiments results in Table 2. This result indicates that, for enhancing the 3D-MoS recognition accuracy, it is important to place the rod at the crossing point of dual-eye sight directions. So it can be concluded that 1000 times inserting has been succeeded since two times recognition enables to detect the positon of object accurately.

Table 4 Recognition error and its standard deviation

	x[mm]	y[mm]	z[mm]
average recognition error	-0.02285	-0.03865	0.030127
standard deviation	0.821726	0.850356	1.360008

4.3 Result for removing experiment

It has been confirmed that the rod can be removed as shown in Fig. 19. The center of sprocket is set at the crossing point of the optical axes of left and right cameras. The movement trajectory of chain is shown in Fig. 20.

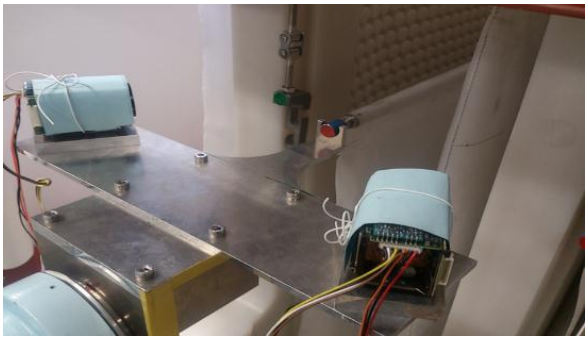

Fig. 19 rod is removed successfully.

At the beginning of removing process that are shown in Fig. 21 (1), the filter cloth rod is recognized and then the robots' hand rise for 30[mm]. Then sprocket model is recognized. If it cannot be recognized, the robots' hands rise for another 30[mm] repeatedly. The rising of the hand will not be stopped until the sprocket can be recognized. Based on the distance from the filter cloth rod to the sprocket model in vertical direction, which can be calculated by their position information achieved by recognition, ---in the case in Fig. 20 the distance is 100[mm]---, the removing of the chain is conducted with an involute function. The process of removing is shown in Fig. 21.

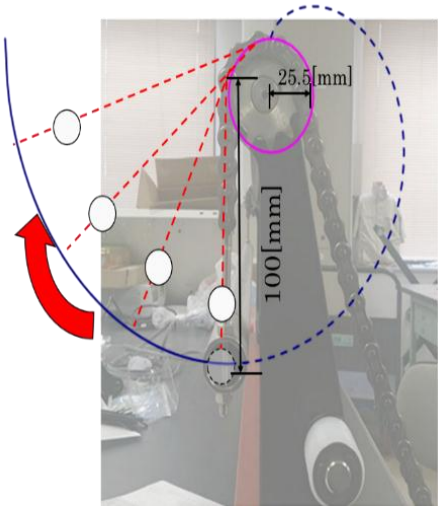

Fig. 20 Pragmatic trajectory pattern of chain removed from sprocket by following involute trajectory.

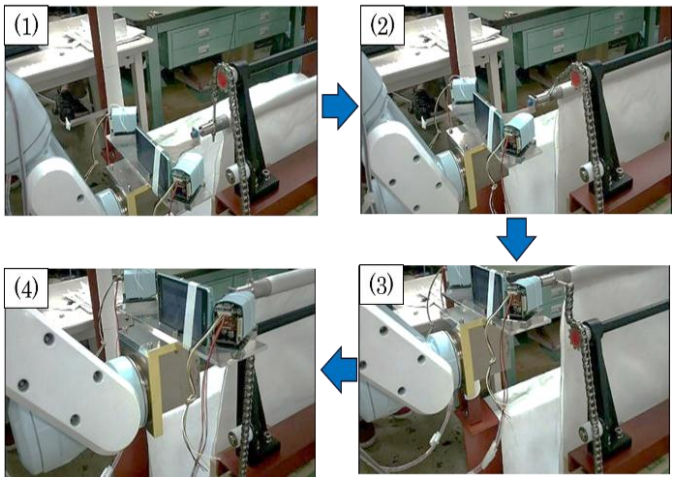

Fig. 21 Remove of chain from sprocket by 3D-MoS controlled cooperative robot system; (1) interdigitation between robot's hand and mandrel end, (2)-(4) removing process of chain from sprocket according to trajectory pattern.

The inserting status of rod and the hole fixed at the top of robot's hand is shown in Fig. 21 (1). The removing of chain from sprocket according to trajectory pattern is shown in Fig. 21 (2)-(4). So it has been confirmed that the chain can be removed by this 3D-MoS system.

5 Conclusion

The "inserting" in the engineering is the most basic and typical pivotal technology about shape synthesis and multi-functionality. It is a process technology that is common in many fields such as aerospace engineering, nuclear engineering, construction engineering, civil engineering industry and so on.

Traditionally, inserting technique has been developed as a high-precision processing technology. The high accuracy "inserting" technology is expected to be applied in unknown or dangerous environment for human beings.

In this research, based on information of color and shape, the filter cloth rod was recognized, inserted and removed by two robots with 3D-MoS system. Then the conclusion can be got as below:

(1) The inserted part of the filter cloth rod was set at the intersection point of the optical axes of left and right cameras. Then, 1000 times recognition experiment was conducted. It was confirmed that the recognition accuracy in x, y, z direction is less than 3mm with the probability of 99.7%.

(2) Based on the result of 1000 times recognition, 1000 times inserting experiment was conducted and all inserting has been succeeded.

(3) The filter cloth rod can be removed from J-hook, and the chain also can be removed by an involute function to generate a trajectory. But it is more difficult to put the rod into J-hook than removing it that requires extreme precision for interconnected motions of two robots. One robot is for fixing the J-hook and the other for gripping the rod and inserting it to the J-hook, in which both robots should avoid conflictions each other. These complex

procedures by two robots incur kinematical coupling problems and constraint force control problems when the rod and J-hook are contacting.

Acknowledgement

We gratefully acknowledge the help of ISHIGAKI COMPANY, LTD, which provided substantial support.

References

[1] ISHIYAMA, S., KAMITANI, M., and KONDO, M.: "New Combination Washing Approach of Chemical Interface Controlled Dispersion and High-Speed Shearing Washing Techniques for Radioactive Contaminated Soil (First Report of Field Test in Fukushima)", Transactions of the Japan Society of Mechanical Engineers, Series B, Vol. 79, No. 802, pp. 1106/1121, 2013

[2] ISHIYAMA, S., KAMITANI, M., KONDO, M., and HIKI, N.: "Reclamation of Highly Radioactive Contaminated Soil by a Combination of Chemical Interface Controlled Dispersion and High-Speed Shearing Washing", Kagaku Kogaku Ronbunshu, Vol. 39, No. 6, pp. 1/8, 2013

[3] ISHIYAMA, S., KAMITANI, M., KONDO, M., and HIKI, N.: "Decontamination of Soil Washing Machines in High Level Radioactive Contaminated Soil Processing by Ceramic Thin Coating with Ion Plating Technique", Kagaku Kogaku Ronbunshu, Vol. 39, No. 4, pp. 1/6, 2013

[4] ISHIYAMA, S., KAMITANI, M., KONDO, M., and HIKI, N.: "Volume Reduction Effect of Radioactive Contaminated Soil by High Temperature Heating Process", Transactions of the Japan Society of Mechanical Engineers, Series A, Vol. 79, No. 805, pp. 1504/1517, 2013

[5] SONG, W., MINAMI, M., YU, F.J., ZHANG, Y.N., and YANOU, A.: "3-D Hand & Eye-Vergence Approaching Visual Servoing with Lyapunouv-Stable Pose Tracking ", IEEE Int. Conf. on Robotics and Automation (ICRA), pp. 5210-5217, 2011.

[6] MAEDA, K., MINAMI, M., YANOU, A., MATSUMOTO, H., YU, F.J., and HOU, S.: "Frequency Response Experiments of 3-D Full Tracking Visual Servoing with Eye-Vergence Hand-Eye Robot System" SICE Annual Conference pp.101-107, 2012.

[7] SONG, W., YU, F.J., and MINAMI, M.: 3D Visual Servoing by Feedforward Evolutionary Recognition, Journal of Advanced Mechanical Design, Systems, and Manufacturing (JSME), Vol.4, No.4, pp.739-755, 2010.